How does canopy height regulate autumn photosynthetic phenology in the Northern Hemisphere?

REPORT

How does canopy height regulate autumn photosynthetic phenology in the Northern Hemisphere?

Rui Tang,[1] Bin He,[1,*] Miaogen Shen,[1] Ziqian Zhong,[2] Hongtao Xu,[1] Tiewei Li,[1] Lanlan Guo,[1] Ling Huang,[1,3] and Xinzi Huang[4]
*Correspondence: hebin@bnu.edu.cn
Received: May 15, 2024; Accepted: September 6, 2024; Published Online: September 29, 2024; https://doi.org/10.59717/j.xinn-geo.2024.100095

GRAPHICAL ABSTRACT

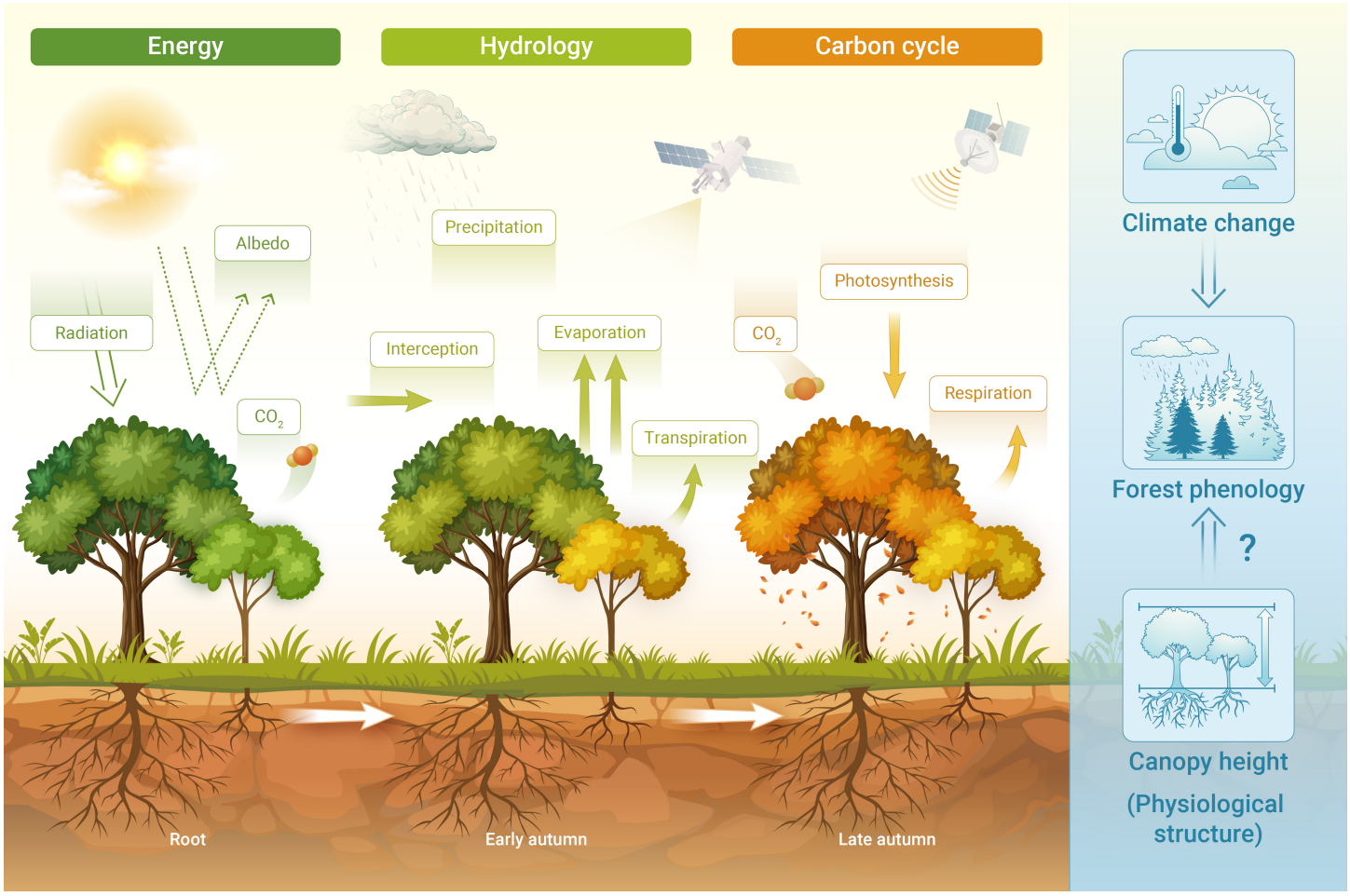

PUBLIC SUMMARY

- We investigated the regulatory effect of forest canopy height on photosynthetic phenology in autumn.
- Widespread (65.2%) positive regulatory of canopy height on the end of growing season in northern forest.
- Canopy height regulates photosynthetic phenology in autumn mainly through radiation and water.
- Considering canopy height may help to improve phenological models.

REPORT

www.the-innovation.org/geoscience

How does canopy height regulate autumn photosynthetic phenology in the Northern Hemisphere?

Rui Tang,[1] Bin He,[1,*] Miaogen Shen,[1] Ziqian Zhong,[2] Hongtao Xu,[1] Tiewei Li,[1] Lanlan Guo,[1] Ling Huang,[1,3] and Xinzi Huang[4]

[1]Faculty of Geographical Science BNU, Beijing Normal University, Beijing 100875, China

[2]Department of Space, Earth and Environment, Division of Geoscience and Remote Sensing, Chalmers University of Technology, Gothenburg SE-412 96, Sweden

[3]College of Urban and Environmental Sciences, Peking University, Beijing 100871, China

[4]Beijing No.4 High School International Campus, Beijing 100031, China

*Correspondence: hebin@bnu.edu.cn

Received: May 15, 2024; Accepted: September 6, 2024; Published Online: September 29, 2024; https://doi.org/10.59717/j.xinn-geo.2024.100095

Citation: Tang R., He B., Shen M., et al., (2024). How does canopy height regulate autumn photosynthetic phenology in the Northern Hemisphere? The Innovation Geoscience **2(4)**: 100095.

Autumn photosynthetic phenology strongly regulates the length of growing season and terrestrial carbon cycle, providing feedbacks to climate change. While the climatic drivers of autumn photosynthetic phenology have received considerable attention, the regulation by forest structural features is frequently overlooked. Here, we used spaceborne LiDAR observations of canopy height, two sets of canopy height products, and satellite solar-induced chlorophyll, to characterize the role of canopy height in autumn photosynthetic phenology from 2001 to 2020. We found strong dependencies of autumn photosynthetic phenology on canopy height in 65.2% of the northern forest. Taller trees tend to end the growing season later, likely due to the enhanced acquisition of solar radiation associated with increased canopy height. Additionally, taller trees have deeper root system to maintain strong hydraulic transport capacity and higher resistance to water stress. This study highlights the importance of forest structure in regulating vegetation phenology and contributes to enhancement of phenological models and carbon cycle simulations.

INTRODUCTION

The seasonal dynamics of terrestrial vegetation strongly regulate the global carbon cycle.[1,2] Precise prediction of vegetation phenology is essential for evaluating vegetation responses and feedbacks to climate change.[3] In recent decades, spring vegetation phenology has significantly advanced across the northern hemisphere due to ongoing global warming.[4] In contrast, the delaying trends in autumn vegetation phenology are less noticeable,[5,6] suggesting greater complexity in the factors governing autumn phenology. Furthermore, increasing evidence suggests that autumn vegetation phenology plays a greater role than spring vegetation phenology in regulating the length of growing season[7] and changes in net ecosystem productivity.[8] Therefore, a better representation of autumn vegetation phenology is urgently required for accurately simulating the effects of climate change on vegetation growth and ecosystem carbon cycle.

Evidence suggests that autumn vegetation phenology is co-dominated by internal vegetation conditions (e.g., metabolic adjustments, genetic expressions),[9] near-surface meteorological factors (e.g., temperature, solar radiation and wind),[10-12] water availability[13,14] and their interactions.[15,16] Despite the complex climatic responses of autumn phenology, it remains unclear how structural features, such as, canopy height, regulate the end of growing season (EOS) processes. Canopy height is a fundamental property of vegetation structure.[17] Its variation significantly affects surface biophysical properties,[18] such as radiation acquisition, thereby affecting surface energy and ultimately the growth and productivity of vegetation.[19-21] Additionally, differences in canopy height result in variations in the biochemical, physiological, and morphological characteristics of vegetation, affecting the efficiency of carbon assimilation and hydraulic behavior.[22,23] These gaps in knowledge cast doubt on the reliable modelling of autumn senescence and ultimately hinder the ability of models to simulate terrestrial carbon sink under future forest changes.

Here, we investigated the regulation of canopy height on EOS in the northern forest (>30°N) and examined its possible mechanism between 2001 and 2020 using satellite products and spaceborne LiDAR data. We assessed the association between canopy height and EOS by using spatially contiguous solar-induced chlorophyll fluorescence (CSIF) satellite datasets as proxy for vegetation autumn photosynthetic phenology, as well as two canopy height products based on spaceborne-lidar data fusion. The regulatory mechanism of canopy height on EOS was explored using the space instead of time method, which included a set of climate factors and biological elements.

MATERIALS AND METHODS

Datasets and study area

We used the clear-sky CSIF dataset with 4-day temporal and 0.05° spatial resolutions to derive the growth cycle of vegetation photosynthesis from 2001 to 2020 in northern ecosystems.[24] It was demonstrated to capture well the seasonal dynamics of satellite-observed SIF, which shows high consistency with ecosystem GPP (gross primary productivity)[25,26] and thus CSIF is suitable for vegetation phenology retrievals as a proxy for GPP.[11]

We focused our study areas on forest in the northern mid-high latitudes (>30°N) during 2000-2020. Here, the forest extent were selected areas that were forest extent both in 2000 and 2020 (Figure S1).[17] The forest canopy height dataset was obtained from the NASA Carbon Monitoring System (CMS) program. This dataset provides estimates of forest canopy height derived from the Geoscience Laser Altimeter System (GLAS) LiDAR instrument that onboard the NASA Ice, Cloud, and land Elevation (ICESat) satellite.[27,28] In this study, we used maximum canopy height to verify the EOS discrepancy under different canopy height. We also used two sets of canopy height products based on spaceborne LiDAR. The Global modeled canopy height distribution map for the year 2005, with a resolution of 1 km, was provided by Simard et al.[29] A lasted 30 m spatial resolution global forest canopy height map for the year 2020 made by a deep learning model based on the fusion of GEDI was provided by Potapov et al.[17]

Elevation data were obtained from Global Multi-resolution Terrain Elevation Data (GMTED) 2010, and the mean elevation data with 30 arc-seconds resolution was selected in this study.

The air temperature dataset were provided by the Climatic Research Unit (CRU ts4.05) with monthly temporal and 0.5° spatial resolutions. The short radiation dataset was provided by the fifth-generation European Centre for Medium-Range Weather Forecasts reanalysis (ERA5-Land) with monthly temporal and 0.1° spatial resolutions. The monthly root-zone soil moisture with a spatial resolution of 0.25° for the period 1980–2020 was obtained from the Global Land Evaporation Amsterdam Model (GLEAM v.3.5a).[30] The 16-day MODIS shortwave albedo product (MCD43C3) comprises black sky and white-sky albedo. Here we refer to the method of Li et al.[31]: simply assume the blue-sky albedo to be the average of black-sky and white-sky albedo. Previous research has demonstrated that EOS is influenced not only by autumn climate, the climate preceding autumn also have a certain impact on EOS,[4] therefore this study selected climate variables from May to September as the indicators of climate variables in the growing season to be used as control variables in the analysis of partial correlation between EOS and canopy height.

The global maximum rooting depth dataset, which has a 1-km spatial resolution, was provided by Fan et al.[32] This dataset is based on the inversion of an ecohydrological model combined with water table estimates, and has been extensively validated by field observations.

Biome data is derived from the Resolve Ecoregions 2017, which serves as

a biogeographic regionalization under an Earth's biomes framework, consisting of 14 terrestrial biomes made up of 846 ecoregions, defining biogeographic assemblages and ecological habitats (Table S1).[33] Climatic region data is procured from the widely utilized Köppen-Geiger climate classification system, which divides the global climate zones into five primary groups based on local vegetation types: tropical, arid, temperate, continental, and polar.[34] Further subdivisions of each group are based on temperature or aridity level (Table S2).

The sap flow dataset was obtained from SAPFLUXNET[35] which is a compiled global plant-level sap flow measurement database. From 194 sites, we selected 40 sites that were located within the study area and provided canopy height information in the observational data. Out of 40 sites, we selected 5 sites that provided observation data for multiple trees of different heights and whose sap flow data were complete enough to extract phenology (Table S3). The day sap density value is obtained by averaging the observed data of sap flow. Then the EOS and corresponding sap flow of each tree were extracted according to phenological extraction method.

Phenology retrieval

We determined EOS using the following three methods: (1) the spline threshold method (Spline-Thr), (2) harmonic analysis of time series maximum rate method (HANTS-Mr), and (3) polynomial fit maximum rate method (Polyfit-Mr).[11] The pixels were selected on the basis of the following criteria: (a) the CSIF values smaller than zero were replaced with zero,[11] (b) an annual maximum CSIF occurs between the July and September.[36] For the spline threshold method, we linearly interpolated the 4-day smoothed CSIF into daily values. The mean seasonal average was calculated, and the minimum value plus 30% of the amplitude was used as the pixel-specific threshold. This threshold was then used for both spring and fall to extract the SOS and EOS. For the HANTS-Mr and Polyfit-Mr methods, we fitted CSIF time-series via "harmonic analysis" and "eight-order polynomial function" and determined the phenology date with maximum increase/decrease in CSIF.[11] The first step involves calculating the multi-year seasonal average using the raw data. Subsequently, change of CSIF at each time step (every 4 days) was calculated, and the dates before the maximum change (positive value) and after the minimum changes (negative value) are selected, and their corresponding CSIF values serve as the thresholds for extracting the SOS and EOS, respectively. The Polyfit-MR method utilizes an eight-order polynomial to predicts the CSIF for each day of the year. Conversely, the HANTS-MR employs a harmonic analysis method for fitted model. Both methods used the thresholds to retrieve the SOS and EOS. Considering that there are certain differences in the extraction phenology of different methods (Figure S2), in order to enhance the credibility of results, subsequent EOS analyses were based on the averages of the values obtained by using the three methods.[37] EOS averages over the five years prior to the year in which the canopy height data were obtained were used to match canopy height.

Before analyses, all datasets were resampled into a unified spatial resolution of 0.05°×0.05° to match the resolution of the CSIF data.

The analysis of EOS - canopy height dependency

We used partial correlation to investigate the relationship between canopy height and EOS. when calculating partial correlation, we controlled for mean growing season temperature, soil moisture, radiation, and DEM, in order to eliminate the influence of environmental factors.

To address potential spatial heterogeneity challenges globally, we employed space instead of time and partition methods to conduct analyses at a finer scale. Firstly, using the method of space instead of time, we selected 11×11 windows to carry out spatial sliding sampling, and conducted partial correlation analysis in each window to explore the relationship between canopy height and EOS, and assigned coefficient to the center grid. Note that only 11×11 windows with more than 30 grid cells with valid EOS values were selected for correlation analysis. Additionally, similar analyses were conducted using 9×9 or 13×13 moving windows to assess result robustness. Besides, we also divided our study area into different regions, including biomes and climatic regions to explore the relationship between canopy height and EOS under different ecological regions and climate types. We then conducted partial correlation analysis on the data within each region.

To validate the analysis results of remote sensing data, we used space-borne LiDAR canopy height data measured at the site to conduct a point-wise analyses. Initially, 4188 canopy height sites for 2005 were selected from a total of 9,825 sites within the study area. Each individual site was then considered as the center, and the Euclidean distance was used to identify nearby sites. Latitude and longitude were used to indicate the coordinates of the point, ensuring that the Euclidean distance between neighboring sites and the central site did not exceed 3°. To further validate the reliability of the results, we also considered Euclidean distances of less than 2° and less than 4°. Outliers, defined as values deviating from the median by more than three times the converted median absolute deviation, were excluded from data within a search window. Subsequently, windows with no fewer than 10 sites were used for subsequent partial correlation analysis. Finally, 1947 central sites were retained, and the partial correlation coefficient was assigned to these central sites.

In addition, to explore the potential mechanisms underlying the regulation of canopy height on EOS, we employed partial correlation analysis at both spatial and point level. Our hypothesis posited that the regulation of canopy height on EOS is mediated by its influence on radiation and water transport. To test this hypothesis, we examined how canopy height regulates radiation reception and water transport, thus affecting EOS.

Effects of different canopy heights on radiation reception

The calculation of clear sky solar radiation is based on the method recommended in the Penman-Monteith formula from the Food and Agriculture Organization of the United Nations (FAO) for the absence of net radiation observations.[38] In this method, the clear sky solar radiation reaching the earth's surface is defined as a unitary linear equation composed of the solar radiation at the top of the atmosphere and the elevation.

$$R_a = 24 \times 60 \times \frac{0.082}{\Pi} \times d_r \times (w_s \times \sin\Phi \times \sin\delta + \cos\Phi\cos\delta\sin w_s) \quad (1)$$

$$d_r = 1 + 0.033 \times \cos\left(\frac{2 \times \Pi}{365} \times J\right) \quad (2)$$

$$w_s = \cos^{-1}(-\tan\Phi\tan\delta) \quad (3)$$

$$\delta = 0.409 \times \sin\left(\frac{2 \times \Pi}{365} \times J - 1.39\right) \quad (4)$$

$$R_{so} = \left(0.75 + \frac{2}{10^5} \times Z\right) \times R_a \quad (5)$$

Where R_a is the solar radiation at the top of the atmosphere, R_{so} is the clear sky solar radiation reaching the surface of the earth, J is the daily number, Φ is the latitude, and Z is the elevation of the calculated point.

As can be seen from formula (5), there is a linear relationship between radiation and height, that is, radiation will increase with the increase of height. Therefore, we hypothesize that increasing canopy height would expose vegetation to more radiation. Therefore, we used the difference between radiation calculated by two heights with and without canopy height to quantification the effects of different canopy heights on the radiation reception of vegetation (hereafter R_{CH}), the radiation calculated without consideration of canopy height was defined as R_{DEM}. Then, we calculate the R_{CH} and EOS differences between the other points in the sliding window and the central point for partial correlation analysis. In addition, in order to further quantify the effects of R_{CH} on EOS without the influence of temperature, moisture and R_{DEM}, we used a ridge regression analysis to verify the effect of R_{CH} on EOS. In the regression analysis, all variables were normalized with z score. Then the proportion of absolute value of regression coefficients to the sum of absolute value of total regression coefficients was used to quantify the influence of each variable on EOS.

RESULTS

Widespread positive regulatory of canopy height on EOS in northern ecosystems

We first used an 11×11 moving window to explore the spatial patterns of partial correlation, aiming to mitigate the influences of temperature, radiation

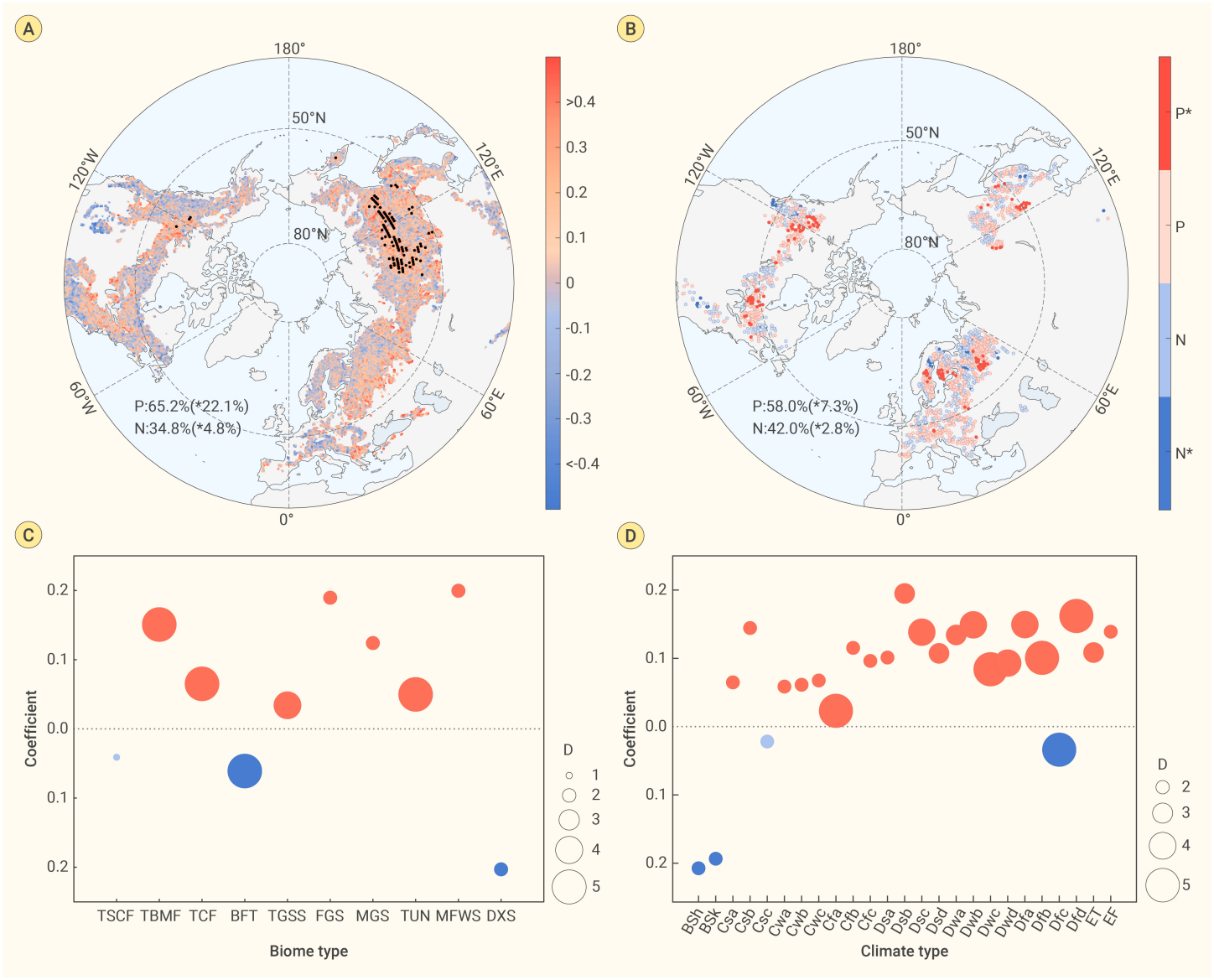

Figure 1. Associations between canopy height and the end of growing season (EOS) north of 30°N (A)(B)The results of the partial correlation analysis between canopy height and EOS from 2001-2005 for satellite data and observation site data. (C)(D) Fractions of partial correlations for canopy height and EOS grouped per biome and climate categories. Regions marked with dots in A have statistically significant ($P < 0.1$) correlation. The legend P and N represents positive coefficient and negative coefficient, *, $P < 0.1$. The size of the circle in C and D represents the number of pixels, red and blue represents a positive correlation and negative correlation, dark color represents a significant correlation, and light color represents an insignificant correlation.

and soil moisture while investigating the regulatory role of canopy height on EOS from 2001 to 2005 (Figure 1A). We found dominantly positive correlation, indicating a later EOS with taller canopy height, in 65.2% of the pixels, primarily located in Central Eurasia. In particular, around quarter (22.1%) of the pixels showed significant (P<0.1) positive correlation between canopy height and EOS. Additionally, partial correlations between canopy height and EOS, calculated using various moving window sizes, EOS extracted by different methods and based on a dataset of canopy height data for 2020 with the average EOS from 2016 to 2020, similar patterns (Figures S3-S5), thereby confirming the robustness of the correlation with canopy height and EOS. Analyses of canopy height observations at the site level revealed similar results, with 7.3% of sites exhibiting a significant (P<0.1) positive correlation between canopy height and EOS, suggesting that the taller canopy heights were associated with later EOS (Figure 1B). Additionally, we conducted analyses using varying search window sizes at site level, yielding consistent results (Figure S6). Since the site data in central Eurasia failed to meet our selection rule and did not show results, we separately analyzed the site data in this region, and selected the data in the same climate region with more than 10 sites through Köppen-Geiger climatic zones, and found that the canopy height and EOS showed a significant positive relationship, consistent with the results in other regions (Figure S7). Furthermore, partial correlation analysis demonstrated consistent findings across forest biomes (Figure 1C) and Köppen-Geiger climatic zones (Figure 1D). For example, significant positive correlations were found in seven out of ten biome types. Conversely, deserts and xeric shrublands (DXS), Boreal Forests/Taiga (BFT) and Tropical & Subtropical Coniferous Forests (TSCF) exhibited negative correlations. Similarly, canopy height and EOS were positively correlated in 21 of 25 climatic zones (all were significant) and negatively correlated in the other four zones (BSh (Arid, steppe, hot), BSk (BSK Arid, steppe, cold), Csc (Temperate, dry summer, cold summer) and Dfc (Cold, no dry season, cold summer)).

Potential Mechanisms of canopy height regulates EOS

Previous research indicates that the primary factors influencing EOS are radiation, temperature and water.[11,13,39] Furthermore, the regulatory of canopy height on EOS may also be influenced by the difference of canopy height on surface biophysical properties. Therefore, we proposed the possible mechanisms by which canopy height regulates EOS, focusing on radiation and water content. We hypothesize that taller forest would receive increased radiation, thereby promoting sustained photosynthesis, and that taller forest may possess deeper roots, enhancing their ability to maintain water and nutrient

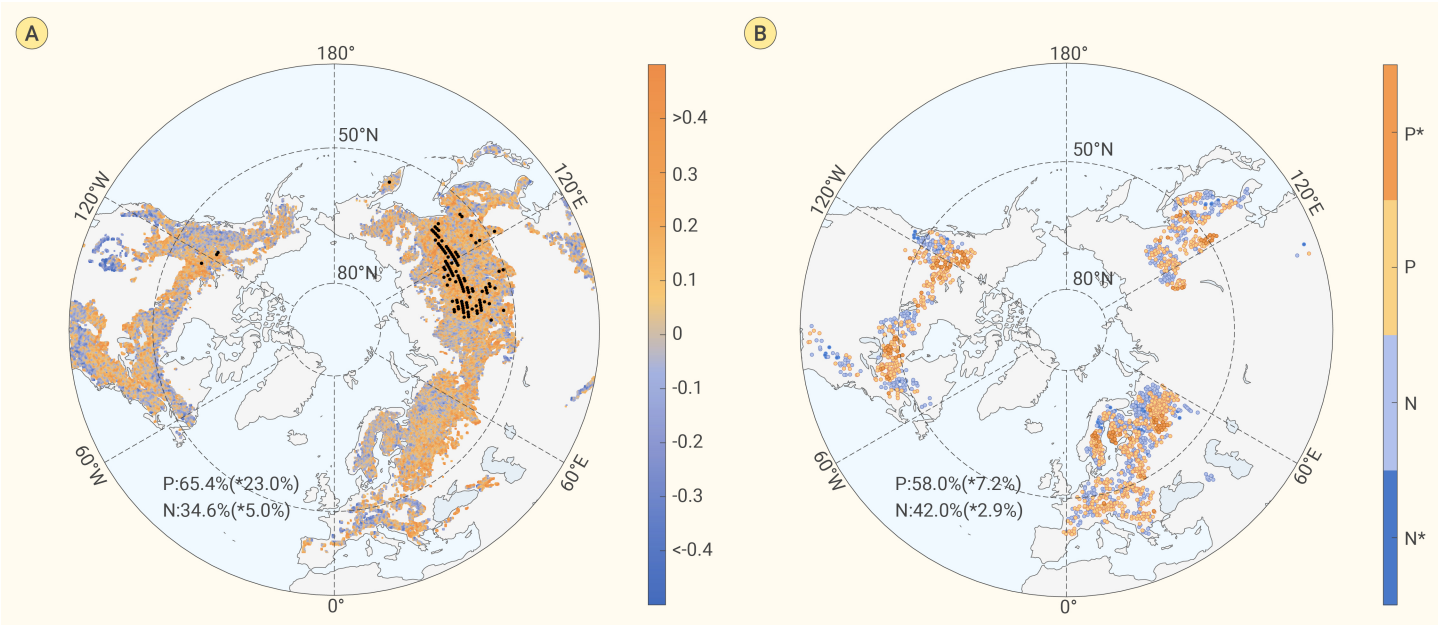

Figure 2. Relationship between the difference of acquired radiation and EOS at different canopy heights A, B, The distribution of the partial correlation coefficient between ΔR_{CH} and ΔEOS from 2001-2005 for satellite and site canopy height. Regions marked with dots in A have statistically significant ($P < 0.1$). The legend P and N represents positive coefficient and negative coefficient, *, $P < 0.1$.

levels in arid or cold climates.

To investigate the possible mechanisms involving radiation, we initially examined the correlation between radiation and EOS in northern forest, revealing a positive correlation in 56.5% of the sites (Figure S8). We emphasize that radiation positively influences EOS, aligning with a recent study that reported radiation's constrain on autumnal photosynthesis.[11] On this foundation, we proceed to investigate how canopy height regulate EOS through radiation. Using the Penman-Monteith formula (see Methods 2.4), we quantified the radiation gain received by vegetation while accounting for canopy height and observed that tall trees captured more solar radiation (Figure S8). To reveal the impact of R_{CH} resulting from canopy height on EOS, we performed a partial correlation analysis and found a positive relationship between ΔR_{CH} and ΔEOS in 65.4% of the pixels (Figure 2A), suggesting that increased radiation due to canopy height may delay EOS. Analysis for site-level canopy height observations yielded consistent results, with 58.0% of sites showing a positive correlation between ΔEOS and ΔR_{CH} (Figure 2B). Similar to the previous analysis of the relationship between canopy height and EOS in central Eurasia, we also conducted a separate analysis of the relationship between ΔR_{CH} and ΔEOS in central Eurasia based on site data, and the results also showed that the increase of R_{CH} had a positive effect on the extension of EOS (Figure S9). Although the amount of radiation increased by canopy height is a small amount for the total radiation received by forest, on the basis of the ridge regression analysis, we found that this small amount of radiation does have an impact on EOS, and the contribution of this impact can be up to about 40% (Figure S10). Despite the modest increment in radiation due to canopy height, it could have several beneficial effects, such as sustaining a longer growth by alleviating radiation limitations and providing better photosynthetic conditions.[5,39]

On the other hand, previous studies have shown that the difference in canopy height will affect the albedo of trees, and the taller the tree, the lower the albedo, which means that trees of different heights will also affect their reception of radiation due to the difference in albedo.[40,41] Therefore, we analyzed the relationship between canopy height and albedo, and found that canopy height and albedo were negatively correlated in 85.2% of the region, that is, the taller the tree, the lower the albedo (Figure S11). This also reaffirms our hypothesis that taller trees can acquire more radiation to maintain EOS.

Water acquisition is primarily facilitated by soil water, which serves as the direct source of water for vegetation growth. The vertical distribution of roots plays a pivotal role in absorbing soil moisture, directly impacting vegetation water supply, and is closely correlated with canopy height.[42] To test this hypothesis, we calculated the partial correlation between canopy height and root depth, grouping them by biome type and climatic zones (Figures 3A-B). The results indicate a predominantly positive relationship between canopy height and root depth. For example, canopy height and root depth were positively correlated in nine out of ten biome types, with seven correlations being significant, while only TSCF showed a negative correlation. Furthermore, 24 out of the 25 climatic zones showed a positive correlation, with 21 correlations being significant, while only Dfd (Cold, no dry season, very cold winter) showed a negative correlation. In addition, we also conducted partial correlation analysis between canopy height and root depth and root depth and EOS in space, and the results showed that forests with higher canopy height tended to have deeper root depth, thus maintaining later EOS (Figure S12). Our results suggest that tall trees tend to have deeper roots, which are conducive to absorbing deeper soil water to cope with water stress and maintain a longer growing season.[43]

We further evaluated the water transport capacity of trees with different canopy heights, as quantified by sap flow density from five sites (Figure 3C), during the corresponding EOS period based on sap flow density. For each site, we calculated the EOS of each tree based on the daily sap flow density and extracted the corresponding sap flow density. The sap flow density values show a positive trend with increasing canopy height across the five sites (Figure 3D), suggesting that tall trees tend to have stronger hydraulic transport capacity, thus providing more favorable conditions for photosynthesis.

DISCUSSION

Efforts have been made to explore the responses of EOS to changes in climate.[44] Here, we provide suggestive evidence that changes in canopy height over the last two decades could have contributed to an overall positive effect on EOS at middle and high latitudes, where site-level and remotely sensed observations indicate that EOS has been extended.[45,46] Both site-level and remotely sensed observations suggest that increased canopy height is associated with a later EOS, and vice versa.

Differences in radiation and hydraulic transport of vegetation due to canopy height are the most probable explanations for the observed positive relationships between canopy height and EOS at about two-thirds of the locations/regions. Taller trees enhance radiation acquisition, as suggested by statistical analysis of remote sensing observations (Figure 2). This study also investigates variations in water acquisition and transport among trees of different canopy heights (Figure 3). It reveals that taller trees have a propensity for accessing deeper soil water[47] and demonstrate stronger water trans-

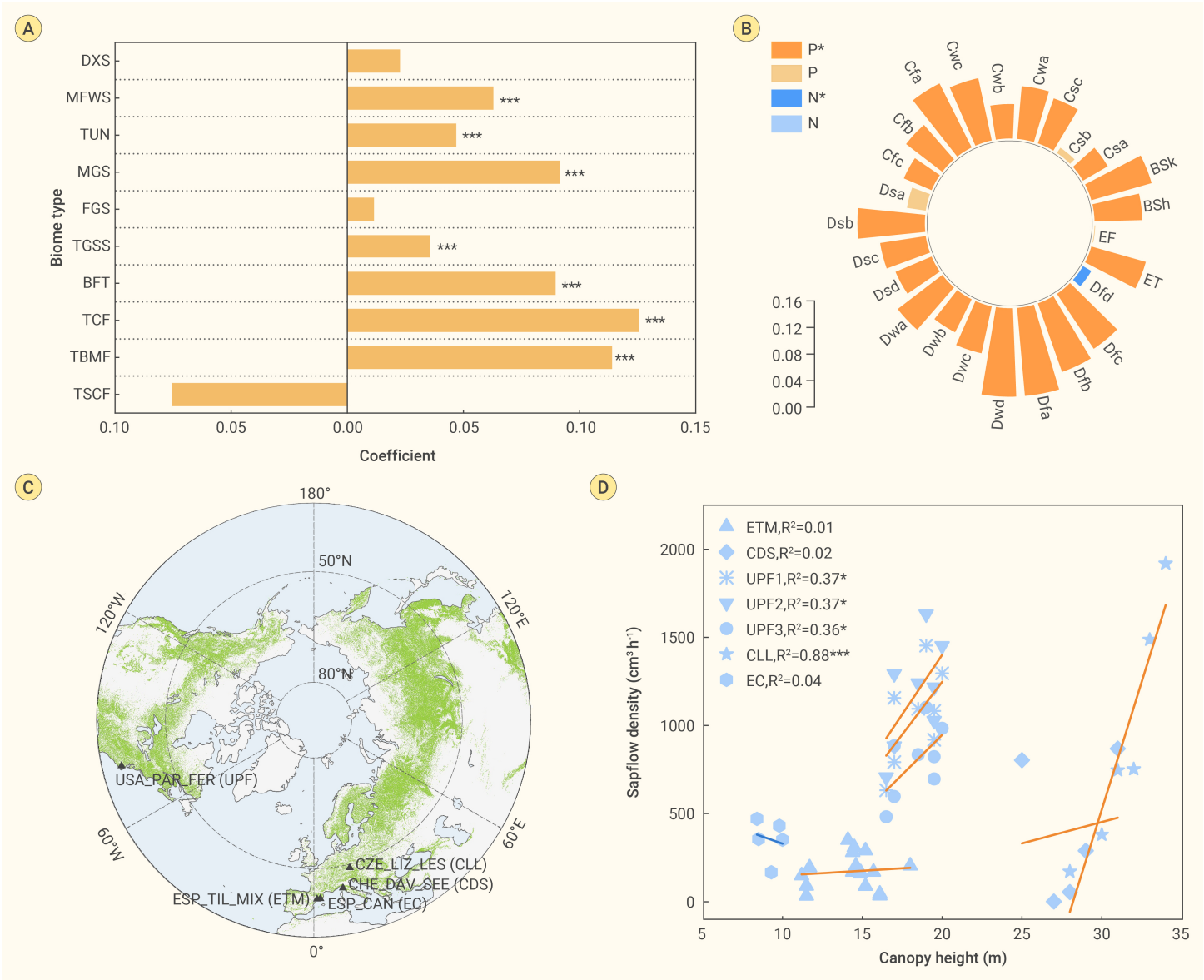

Figure 3. Relationship between canopy height and water transport variables affecting EOS (A)(B) Partial correlations between canopy height and root depth grouped by biome type and climatic zones. (C) The spatial distribution of five sap flow sites. (D) Relationship between canopy height and sap flow density during each EOS. The one asterisk and three asterisks in A and D indicate the statistical significance level of $P<0.1$ and $P<0.01$. The legend P and N in B represents positive coefficient and negative coefficient, *, $P < 0.1$. The symbol in D represents different site-year, the solid line represents the relationship fitting line, the orange represents the positive relationship, and the blue represents the negative relationship.

port capabilities to cope with water stress.[48] The later EOS of taller vegetation may also be attributed to the advantages of taller vegetation's own structure and environment. Taller trees tend to have higher photosynthesis rates and larger canopies.[49] Larger canopies help trap precipitation[50] and capture more water for tree growth (Figure 4).

Nearly one-third of satellite and site data with correlations between canopy height and EOS had negative values, implying that a shorter canopy height may result in a later EOS. This could be because tall trees have greater resistance to air,[51] reducing wind speed at the surface, then the short trees could reduce the evapotranspiration and soil water loss, and also reduced risk from frost disaster (Figure 4).[10,12] Our findings also revealed that the majority of negative canopy height-EOS correlations were distributed in cold regions or arid regions (Figure 1C-D), indicating that frost disaster and water stress might counteract the positive regulation of tall canopy height and accelerate EOS of tall trees.

Vegetation phenology plays a crucial role in both climate change and the carbon cycle. Existing phenology research and model development primarily rely on climate variables, neglecting sufficient consideration of vegetation's physiological structure. The canopy height would have significant regulation on vegetation phenology, and these consequences for regional and global carbon uptake may also be as important as that from variations in climate variables. While the canopy height products have limitations, the general results of our analysis are credible because the relative changes of canopy height were employed rather than absolute values. We found that EOS would be delayed with larger canopy height than shorter one, which mainly regulated by the radiation acquisition. Given that the EOS has been closely linked with annual carbon uptake,[8] a later EOS projected would produce negative feedback, necessitating our attention and proper representation in future ecosystem models. Furthermore, wildfires and logging are common disruptions in forested areas,[52] which have a significant impact on tree canopy height in the short term. As a result, it is crucial to assess the potential long-term effects of these disruptions on the EOS and terrestrial carbon cycle, as they have a direct impact on canopy height.

REFERENCES

1. Piao, S., Ciais, P., Friedlingstein, P., et al. (2008). Net carbon dioxide losses of northern ecosystems in response to autumn warming. Nature **451**: 49–52. DOI: 10.1038/nature06444.
2. Piao, S., Liu, Q., Chen, A., et al. (2019). Plant phenology and global climate change:

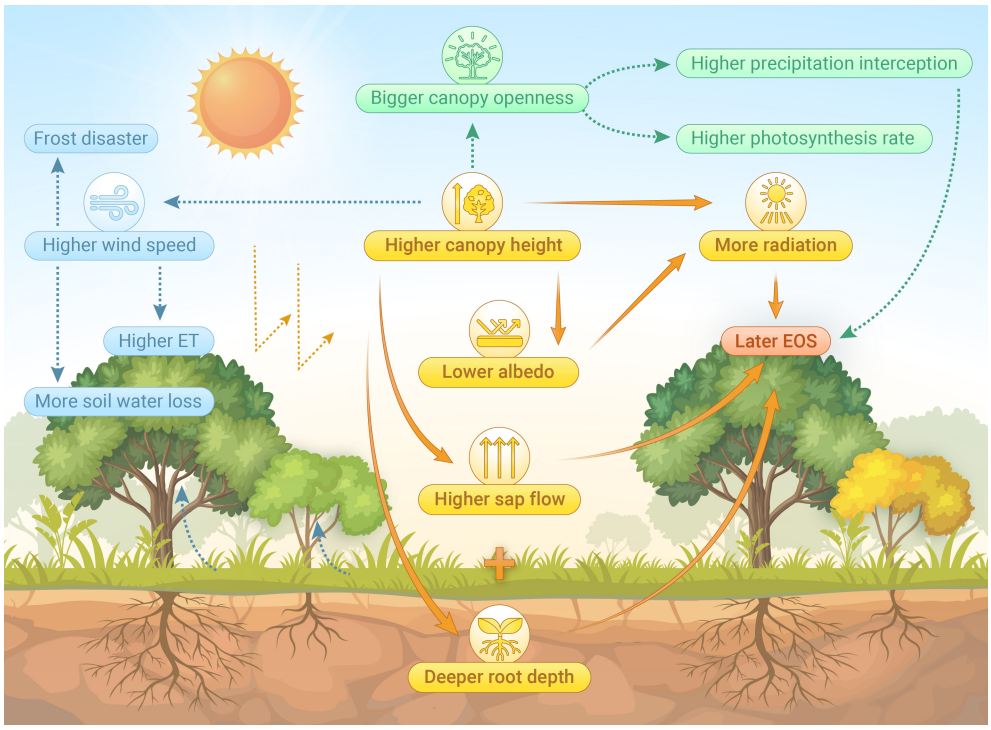

Figure 4. Conceptual illustrations of the effect with different canopy heights on EOS.

Current progresses and challenges. Glob. Chang. Biol. **25**: 1922-1940. DOI: 10.1111/gcb.14619.

3. Li, S., Wang, Y., Ciais, P., et al. (2022). Deficiencies of phenology models in simulating spatial and temporal variations in temperate spring leaf phenology. J. Geophys. Res.: Biogeosciences **127**: e2021JG006421. DOI: 10.1029/2021JG006421.
4. Jeong, S.-J., Ho, C.-H., Gim, H.-J., et al. (2011). Phenology shifts at start vs. end of growing season in temperate vegetation over the Northern Hemisphere for the period 1982-2008. Glob. Chang. Biol. **17**: 2385-2399. DOI: 10.1111/j.1365-2486.2011.02397.x.
5. Liu, Q., Fu, Y.H., Zeng, Z., et al. (2016). Temperature, precipitation, and insolation effects on autumn vegetation phenology in temperate China. Glob. Chang. Biol. **22**: 644–655. DOI: 10.1111/gcb.13081.
6. Wang, M., Li, P., Peng, C., et al. (2022). Divergent responses of autumn vegetation phenology to climate extremes over northern middle and high latitudes. Glob. Ecol. Biogeogr. **31**: 2281-2296. DOI: 10.1111/geb.13583.
7. Garonna, I., de Jong, R., de Wit, A.J.W., et al. (2014). Strong contribution of autumn phenology to changes in satellite-derived growing season length estimates across Europe (1982–2011). Glob. Chang. Biol. **20**: 3457-3470. DOI: 10.1111/gcb.12625.
8. Wu, C., Chen, J.M., Black, T.A., et al. (2013). Interannual variability of net ecosystem productivity in forests is explained by carbon flux phenology in autumn. Glob. Ecol. Biogeogr. **22**: 994–1006. DOI: 10.1111/geb.12044.
9. Lim, P.O., Kim, H.J., and Nam, H.G. (2007). Leaf senescence. Annu. Rev. Plant Biol. **58**: 115–136. DOI: 10.1146/annurev.arplant.57.032905.105316.
10. Wu, C., Wang, J., Ciais, P., et al. (2021). Widespread decline in winds delayed autumn foliar senescence over high latitudes. Proc. Natl. Acad. Sci. USA **118**: e2015821118. DOI: 10.1073/pnas.2015821118.
11. Zhang, Y., Commane, R., Zhou, S., et al. (2020). Light limitation regulates the response of autumn terrestrial carbon uptake to warming. Nat. Clim. Change. **10**: 739–743. DOI: 10.1038/s41558-020-0806-0.
12. Liu, Q., Piao, S., Janssens, I.A., et al. (2018). Extension of the growing season increases vegetation exposure to frost. Nat. Commun. **9**: 426. DOI: 10.1038/s41467-017-02690-y.
13. Wu, C., Peng, J., Ciais, P., et al. (2022). Increased drought effects on the phenology of autumn leaf senescence. Nat. Clim. Change. **12**: 943–949. DOI: 10.1038/s41558-022-01464-9.
14. Wang, X., Wu, C., Liu, Y., et al. (2023). Earlier leaf senescence dates are constrained by soil moisture. Glob. Change Biol. **29**: 1557-1573. DOI: 10.1111/gcb.16569.
15. Buitenwerf, R., Rose, L., and Higgins, S.I. (2015). Three decades of multi-dimensional change in global leaf phenology. Nat. Clim. Change. **5**: 364–368. DOI: 10.1038/nclimate2533.
16. Deslauriers, A. and Rossi, S. (2019). Metabolic memory in the phenological events of plants: Looking beyond climatic factors. Tree Physiol. **39**: 1272–1276. DOI: 10.1093/treephys/tpz082.
17. Potapov, P., Li, X., Hernandez-Serna, A., et al. (2021). Mapping global forest canopy height through integration of GEDI and Landsat data. Remote Sens. Environ. **253**: 112165. DOI: 10.1016/j.rse.2020.112165.
18. Kumkar, Y., Astrup, R., Stordal, F., et al. (2020). Quantifying regional surface energy responses to forest structural change in Nordic Fennoscandia. J. Geophys. Res. Atmos. **125**: e2019JD032092. DOI: 10.1029/2019JD032092.
19. Kuusinen, N., Tomppo, E., Shuai, Y., et al. (2014). Effects of forest age on albedo in boreal forests estimated from MODIS and Landsat albedo retrievals. Remote Sens. Environ. **145**: 145-153. DOI: 10.1016/j.rse.2014.02.005.
20. Xu, P., Zhou, T., Zhao, X., et al. (2018). Diverse responses of different structured forest to drought in Southwest China through remotely sensed data. Int. J. Appl. Earth Obs. Geoinf. **69**: 217-225. DOI: 10.1016/j.jag.2018.03.009.
21. Moon, M., Li, D., Liao, W., et al. (2020). Modification of surface energy balance during springtime: The relative importance of biophysical and meteorological changes. Agric. For. Meteorol. **284**: 107905. DOI: 10.1016/j.agrformet.2020.107905.
22. Lindroth, A. and Cienciala, E. (1996). Water use efficiency of short-rotation Salix viminalis at leaf, tree and stand scales. Tree Physiol. **16**: 257–262. DOI: 10.1093/treephys/16.1-2.257%JTreePhysiology.
23. Binkley, D., Campoe, O.C., Gspaltl, M., et al. (2013). Light absorption and use efficiency in forests: Why patterns differ for trees and stands. For. Ecol. Manag. **288**: 5-13. DOI: 10.1016/j.foreco.2011.11.002.
24. Zhang, Y., Joiner, J., Alemohammad, S.H., et al. (2018). A global spatially contiguous solar-induced fluorescence (CSIF) dataset using neural networks. Biogeosciences **15**: 5779–5800. DOI: 10.5194/bg-15-5779-2018.
25. Guanter, L., Zhang, Y., Jung, M., et al. (2014). Global and time-resolved monitoring of crop photosynthesis with chlorophyll fluorescence. Proc. Natl Acad. Sci. USA **111**: E1327–1333. DOI: 10.1073/pnas.1320008111.
26. Sun, Y., Frankenberg, C., Wood, J.D., et al. (2017). OCO-2 advances photosynthesis observation from space via solar-induced chlorophyll fluorescence. Science **358**: eaam5747. DOI: 10.1126/science.aam5747.
27. Healey, S.P., Hernandez, M.W., Edwards, D.P., et al. (2015). CMS: GLAS LiDAR-derived global estimates of forest canopy height, 2004-2008. ORNL Distributed Active Archive Center. http://dx.doi.org/10.3334/ORNLDAAC/1271
28. Lefsky, M.A., Keller, M., Pang, Y., et al. (2007). Revised method for forest canopy height estimation from Geoscience Laser Altimeter System waveforms. J. Appl. Remote Sens. **1**: 013537-013518. DOI: 10.1117/1.2795724.
29. Simard, M., Pinto, N., Fisher, J.B., et al. (2011). Mapping forest canopy height globally with spaceborne lidar. J. Geophys. Res. **116**: G04021. DOI: 10.1029/2011jg001708.
30. Martens, B., Miralles, D.G., Lievens, H., et al. (2017). GLEAM v3: Satellite-based land evaporation and root-zone soil moisture. Geosci. Model Dev. **10**: 1903–1925. DOI: 10.5194/gmd-10-1903-2017.
31. Li, Y., Zhao, M., Motesharrei, S., et al. (2015). Local cooling and warming effects of forests based on satellite observations. Nat. Commun. **6**: 6603. DOI: 10.1038/ncomms7603.
32. Fan, Y., Miguez-Macho, G., Jobbagy, E.G., et al. (2017). Hydrologic regulation of plant rooting depth. Proc. Natl. Acad. Sci. USA **114**: 10572–10577. DOI: 10.1073/pnas.1712381114.
33. Dinerstein, E., Olson, D., Joshi, A., et al. (2017). An ecoregion-based approach to protecting half the terrestrial realm. Bioscience **67**: 534–545. DOI: 10.1093/biosci/bix014.
34. Beck, H.E., Zimmermann, N.E., McVicar, T.R., et al. (2018). Present and future Köppen-Geiger climate classification maps at 1-km resolution. Sci. Data **5**: 180214. DOI: 10.1038/sdata.2018.214.
35. Poyatos, R., Granda, V., Molowny-Horas, R., et al. (2016). SAPFLUXNET: Towards a global database of sap flow measurements. Tree Physiol. **36**: 1449–1455. DOI: 10.1093/treephys/tpw110.
36. Shen, M., Tang, Y., Chen, J., et al. (2011). Influences of temperature and precipitation before the growing season on spring phenology in grasslands of the central and eastern Qinghai-Tibetan Plateau. Agric. For. Meteorol. **151**: 1711–1722. DOI: 10.1016/j.agrformet.2011.07.003.
37. Meng, F., Felton, A.J., Mao, J., et al. (2024). Consistent time allocation fraction to vegetation green-up versus senescence across northern ecosystems despite recent climate change. Sci. Adv. **10**: eadn2487. DOI:10.1126/sciadv.adn2487.
38. Allen, R.G., Pereira, L.S., Raes, D., et al. (1998). Crop evapotranspiration - Guidelines for computing crop water requirements - FAO Irrigation and drainage paper 56.
39. Liu, Q., Fu, Y.H., Zhu, Z., et al. (2016). Delayed autumn phenology in the Northern

Hemisphere is related to change in both climate and spring phenology. Glob. Chang. Biol. **22**: 3702–3711. DOI: 10.1111/gcb.13311.
40. Kempes, C.P., West, G.B., Crowell, K., and Girvan, M. (2011). Predicting maximum tree heights and other traits from allometric scaling and resource limitations. PLoS One **6**: e20551. DOI: 10.1371/journal.pone.0020551.
41. Halim, M.A., Chen, H.Y.H., and Thomas, S.C. (2019). Stand age and species composition effects on surface albedo in a mixedwood boreal forest. Biogeosciences **16**: 4357–4375. DOI: 10.5194/bg-16-4357-2019.
42. Schenk, H.J. and Jackson, R.B. (2002). Rooting depths, lateral root spreads and below-ground/above-ground allometries of plants in water-limited ecosystems. J. Ecol. **90**: 480-494. DOI: 10.1046/j.1365-2745.2002.00682.x.
43. Chunxia, H., Jiyue, L., Ming, G., et al. (2008). Changes in leaf photosynthetic characteristics and water use efficiency along with tree height of 4 tree species. Acta Ecol. Sin. **28**: 3008-3016. DOI: 10.1016/S1872-2032(08)60064-5.
44. Zhu, Z., Piao, S., Myneni, R.B., et al. (2016). Greening of the Earth and its drivers. Nat. Clim. Change. **6**: 791–795. DOI: 10.1038/nclimate3004.
45. Richardson, A.D., Keenan, T.F., Migliavacca, M., et al. (2013). Climate change, phenology, and phenological control of vegetation feedbacks to the climate system. Agric. For. Meteorol. **169**: 156–173. DOI: 10.1016/j.agrformet.2012.09.012.
46. Zhu, W., Tian, H., Xu, X., et al. (2012). Extension of the growing season due to delayed autumn over mid and high latitudes in North America during 1982–2006. Glob. Ecol. Biogeogr. **21**: 260-271. DOI: 10.1111/j.1466-8238.2011.00675.x.
47. Martínez-Vilalta, J. and Garcia-Forner, N. (2017). Water potential regulation, stomatal behaviour and hydraulic transport under drought: deconstructing the iso/anisohydric concept. Plant Cell Environ. **40**: 962-976. DOI: 10.1111/pce.12846.
48. Rowland, L., da Costa, A.C.L., Galbraith, D.R., et al. (2015). Death from drought in tropical forests is triggered by hydraulics not carbon starvation. Nature **528**: 119–122. DOI: 10.1038/nature15539.
49. Rijkers, T., Pons, T.L., and Bongers, F. (2000). The effect of tree height and light availability on photosynthetic leaf traits of four neotropical species differing in shade tolerance. Funct. Ecol. **14**: 77-86. DOI: 10.1046/j.1365-2435.2000.00395.x.
50. Yang, B., Lee, D.K., Heo, H.K., et al. (2019). The effects of tree characteristics on rainfall interception in urban areas. Landsc. Ecol. Eng. **15**: 289–296. DOI: 10.1007/s11355-019-00383-w.
51. Bonan, G. (2015). Ecological climatology: concepts and applications, 3 Edition (Cambridge University Press). DOI: 10.1017/CBO9781107339200. https://www.cambridge.org/core/books/ecological-climatology/D146443B007985BC366B2512345692C0.
52. Curtis, P.G., Slay, C.M., Harris, N.L., et al. (2018). Classifying drivers of global forest loss. Science **361**: 1108–1111. DOI: 10.1126/science.aau3445.

FUNDING AND ACKNOWLEDGMENTS

This work was funded by State Key Laboratory of Earth Surface Processes and Resource Ecology (Beijing Normal University) (2023-KF-02). No conflict of interest exits in the submission of this manuscript, and manuscript is approved by all authors for publication. I would like to declare on behalf of my co- authors that the work described was original research that has not been published previously, and not under consideration for publication elsewhere, in whole or in part. The founders had no role in study design, data collection and analysis, decision to publish, or preparation of the manuscript.

AUTHOR CONTRIBUTIONS

Bin He designed the study. Rui Tang collected the data, performed data analyses and wrote the initial manuscript. All authors contributed to the results interpretation and manuscript polishing.

DECLARATION OF INTERESTS

The authors declare no competing interests.

DATA AND CODE AVAILABILITY

All datasets that support the findings of this study are publicly available.The forest extent and the canopy height dataset for the year 2020 are from https://glad.umd.edu/dataset/GLCLUC2020. The canopy height dataset forthe year 2005 is from https://landscape.jpl.nasa.gov. The canopy heightdataset of forest sites is from https://daac.ornl.gov/CMS/guides/LIDAR_FOREST_CANOPY_HEIGHTS.html. The CSIF dataset is from https://doi.org/10.17605/OSF.IO/8XQY6. The land cover type dataset is from https://lpdaac.usgs.gov/products/mcd12c1v006/. The air temperature dataset is from https://crudata.uea.ac.uk/cru/data/hrg/?_ga=2.59088362.697252133.1709108798-447902937.1695218161. The root-zone soil moisture dataset is from https://www.gleam.eu/. The surface solar radiation downwards datasets is from https://cds.climate.copernicus.eu/cdsapp#!/dataset/reanalysis-era5-land?tab=form. The sap flow density data set was obtained from sap flowmeasurements (SAPFLUXNET: https://zenodo.org/record/3697807#Xs4yo4gza5u). The elevation dataset is from https://www.usgs.gov/coastal-changes-and-impacts/gmted2010. The global maximum rooting depth offorests was obtained from Fan et al. (2017) (https://wci.earth2observe.eu/thredds/catalog/usc/root-depth/catalog.html). The Köppen-Geigerclimate classification dataset is from https://www.gloh2o.org/koppen/. The biome typedataset is from https://ecoregions.appspot.com/. The albedo dataset is from https://lpdaac.usgs.gov/products/mcd43c3v061/.

All computer codes for the analysis of the data are available from the corresponding author on reasonable request.

SUPPLEMENTAL INFORMATION

It can be found online at https://doi.org/10.59717/j.xinn-geo.2024.100095.